1-1-2010

ESI-MS and thermal melting studies of nanoscale platinum(ii) metallomacrocycles with DNA

Margaret M. Harding

Louis M. Rendina
University of Sydney

David Schilter
University of Sydney

Thitima Urathamakul
University of Wollongong, thitima@uow.edu.au

Jennifer L. Beck
University of Wollongong, jbeck@uow.edu.au

ESI-MS and thermal melting studies of nanoscale platinum(ii) metallomacrocycles with DNA

Abstract

The hydrophilic, long-chain diamine PEGda (O,O'-bis(2-aminoethyl)octadeca(ethylene glycol)), when complexed with cis-protected Pt(II) ions afforded water-soluble complexes of the type [Pt(N,N)(PEGda)](NO3)2 (N,N = N,N,N',N'-tetramethyl-1,2-diaminoethane (tmeda), 1,2-diaminoethane (en), and 2,2'-bipyridine (2,2'-bipy)) featuring unusual 62-membered chelate rings. Equimolar mixtures containing either the 16-mer duplex DNA D2 or the single-stranded D2a and [Pt(N,N)(PEGda)]2+ were analyzed by negative-ion ESI-MS. Analysis of D2-Pt(II) mixtures showed the formation of 1:1 adducts of [Pt(en)(PEGda)]2+, [Pt(tmeda)(PEGda)]2+ and the previously-described metallomacrocycle [Pt2(2,2'-bipy)2{4,4'-bipy(CH2)44,4'-bipy}2]8+ with D2; the dinuclear species bound to D2 most strongly, consistent with its greater charge and aromatic surface area. D2 formed 1:2 complexes with the acyclic species [Pt(2,2'-bipy)(Mebipy)2]4+ and [Pt(2,2'-bipy)(NH3)2]2+. Analyses of D2a-Pt(II) mixtures gave results similar to those obtained with D2, although fragmentation was more pronounced, indicating that the nucleobases in D2a play more significant roles in mediating the decomposition of complexes than those in D2, in which they are paired in a complementary manner. Investigations were also conducted into the effects of selected platinum(II) complexes on the thermal denaturation of calf thymus DNA (CT-DNA) in buffered solution. Both [Pt2(2,2'-bipy)2{4,4'-bipy(CH2)64,4'-bipy}2]8+ and [Pt(2,2'-bipy)(Mebipy)2]4+ stabilized CT-DNA. In contrast, [Pt(tmeda)(PEGda)]2+ and [Pt(en)(PEGda)]2+ (as well as free PEGda) caused negligible changes in melting temperature (ΔTm), suggesting that these species interact weakly with CT-DNA.

Keywords

ms, esi, studies, melting, nanoscale, thermal, platinum, ii, metallomacrocycles, dna, CMMB

Disciplines

Life Sciences | Physical Sciences and Mathematics | Social and Behavioral Sciences

Publication Details

Harding, M. M., Rendina, L. M., Schilter, D., Urathamakul, T. & Beck, J. L. (2010). ESI-MS and thermal melting studies of nanoscale platinum(ii) metallomacrocycles with DNA. Dalton Transactions, 39 (46), 11263-11271.

ESI-MS and thermal melting studies of nanoscale platinum(II) metallomacrocycles with DNA

David Schilter,[a] Thitima Urathamakul,[b] Jennifer L. Beck,[b] Margaret M. Harding[c] and Louis M. Rendina*[a]

Received 30th June 2010, Accepted 3rd September 2010
DOI: 10.1039/c0dt00754d

The hydrophilic, long-chain diamine PEGda (*O*,*O*′-bis(2-aminoethyl)octadeca(ethylene glycol)), when complexed with *cis*-protected Pt(II) ions afforded water-soluble complexes of the type $[Pt(N,N)(PEGda)](NO_3)_2$ (*N*,*N* = *N*,*N*,*N*′,*N*′-tetramethyl-1,2-diaminoethane (tmeda), 1,2-diaminoethane (en), and 2,2′-bipyridine (2,2′-bipy)) featuring unusual 62-membered chelate rings. Equimolar mixtures containing either the 16-mer duplex DNA **D2** or the single-stranded **D2a** and $[Pt(N,N)(PEGda)]^{2+}$ were analyzed by negative-ion ESI-MS. Analysis of **D2**-Pt(II) mixtures showed the formation of 1 : 1 adducts of $[Pt(en)(PEGda)]^{2+}$, $[Pt(tmeda)(PEGda)]^{2+}$ and the previously-described metallomacrocycle $[Pt_2(2,2'\text{-bipy})_2\{4,4'\text{-bipy}(CH_2)_4 4,4'\text{-bipy}\}_2]^{8+}$ with **D2**; the dinuclear species bound to **D2** most strongly, consistent with its greater charge and aromatic surface area. **D2** formed 1 : 2 complexes with the acyclic species $[Pt(2,2'\text{-bipy})(Mebipy)_2]^{4+}$ and $[Pt(2,2'\text{-bipy})(NH_3)_2]^{2+}$. Analyses of **D2a**-Pt(II) mixtures gave results similar to those obtained with **D2**, although fragmentation was more pronounced, indicating that the nucleobases in **D2a** play more significant roles in mediating the decomposition of complexes than those in **D2**, in which they are paired in a complementary manner. Investigations were also conducted into the effects of selected platinum(II) complexes on the thermal denaturation of calf thymus DNA (CT-DNA) in buffered solution. Both $[Pt_2(2,2'\text{-bipy})_2\{4,4'\text{-bipy}(CH_2)_6 4,4'\text{-bipy}\}_2]^{8+}$ and $[Pt(2,2'\text{-bipy})(Mebipy)_2]^{4+}$ stabilized CT-DNA. In contrast, $[Pt(tmeda)(PEGda)]^{2+}$ and $[Pt(en)(PEGda)]^{2+}$ (as well as free PEGda) caused negligible changes in melting temperature (ΔT_m), suggesting that these species interact weakly with CT-DNA.

Introduction

The binding of small molecules to DNA, both in terms of fundamental chemistry as well as drug design, is a topic of intense research activity.[1–4] Organic compounds and mono- and di-nuclear metal complexes[5,6] have provided a wealth of insight into the way small molecules interact with DNA *via* non-covalent minor and major groove binding, intercalation, and electrostatic interactions, as well as *via* the formation of covalent adducts.

A number of recent studies have highlighted the potential of metallosupramolecular architectures to exhibit new modes of DNA-binding and biological activity not previously observed with other synthetic systems. For example, a diiron(II) triple helicate has been shown to bind to natural DNA as well as the palindromic hexanucleotide 5′-CGTACG-3′.[7] In the latter case, X-ray analysis of single crystals obtained from the helicate-oligonucleotide complex revealed the presence of a three-way DNA junction, rather than the expected duplex DNA. In an exquisite example of molecular recognition and guest-promoted self-assembly, the triple-helicate guest occupied the central cavity of the DNA host, undoubtedly stabilising the Y-junction motif.

Recent studies on the interactions of metallomacrocycles with nucleic acids also suggest that metallomacrocycles are a potential novel class of DNA-binding compounds that possess unusual DNA-binding features and biological properties. The molecular square $[Pt_4(en)_4(4,4'\text{-bipy})_4](NO_3)_8$ (**1**·8NO_3) significantly affects the secondary and tertiary structures of DNA, causes apoptosis and displays a cytotoxicity comparable to that of cisplatin against the HL-60 leukaemia cell line.[8] $\mathbf{1}^{8+}$ also effectively binds to a G-quadruplex and inhibits telomerase,[9] an enzyme that aids in the protection of chromosomes and is overexpressed in *ca.* 85% of all cancers.[10] A related complex, the platinum(II) 'metallacalixarene' $\mathbf{2}^{4+}$, binds mononucleotides[11] and interacts non-covalently with calf thymus DNA (CT-DNA). At low concentrations of $\mathbf{2}^{4+}$, DNA supercoiling was observed, whereas atomic force microscopy imaging demonstrated that the DNA uncoiled into long, rigid structures in the presence of high concentrations of the metal complex.[12] Very recently, the tetranuclear ruthenium(II) metallomacrocycle **3** has been reported to interact with duplex DNA with an affinity several orders of magnitude higher than its mononuclear building blocks, producing large scale bending of DNA.[13]

Herein we report the synthesis of a series of mononuclear, 62-membered, cationic metallomacrocycles **4**·2NO_3 – **6**·2NO_3 containing a highly flexible polyethylene glycol linker; we recently reported the synthesis and characterisation of a number of highly cationic metallomacrocyclic Pd(II) and Pt(II) complexes, *e.g.* $\mathbf{8}^{8+}$ and $\mathbf{9}^{8+}$, containing ligands that incorporate two positively-charged *N*-heterocycles linked by a conformationally-flexible spacer unit.[14] These metallomacrocycles possess high aqueous

[a]*School of Chemistry, The University of Sydney, Sydney, NSW, 2006, Australia. E-mail: lou.rendina@sydney.edu.au; Fax: 61 2 9351 3329; Tel: 61 2 9351 4781*
[b]*School of Chemistry, The University of Wollongong, Wollongong, NSW, 2522, Australia*
[c]*School of Chemistry, The University of New South Wales, Sydney, NSW, 2052, Australia*

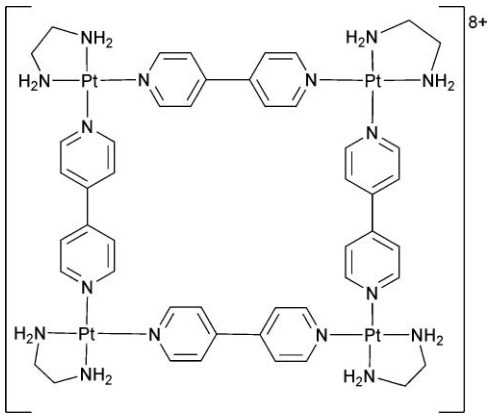

1

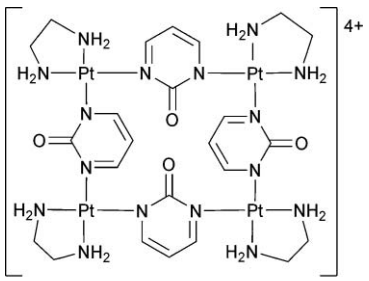

2

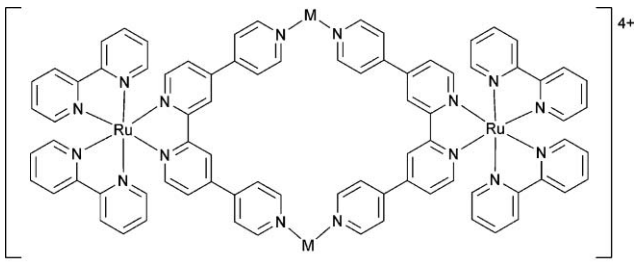

3 M = [ReCl(CO)$_3$]

solubility and charge and contain cavities which are semi-rigid and of nanoscale dimensions. The DNA-binding characteristics of both these classes of complexes with double- and single-stranded DNA (dsDNA and ssDNA, respectively) were investigated using ESI-MS and thermal denaturation experiments. These metallomacrocycles differ from those previously studied with DNA with respect to their level of positive charge and the presence of flexible ($\mathbf{4}^{2+}$ – $\mathbf{6}^{2+}$) and semi-rigid ($\mathbf{8}^{8+}$ and $\mathbf{9}^{8+}$) nanoscale cavities. These species can adopt conformations with a variety of shapes and dimensions that may recognise different features of ssDNA and/or dsDNA. In addition, the large cavities allow for a possible topological interaction by encircling DNA in a non-covalent manner much like the natural toroidal proteins such as DNA sliding clamp proteins.[15,16]

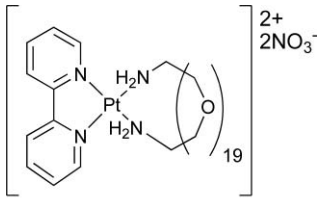

4·2NO$_3$

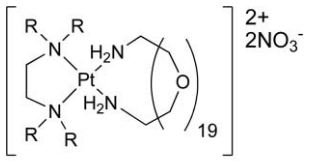

5·2NO$_3$ (R = Me)
6·2NO$_3$ (R = H)

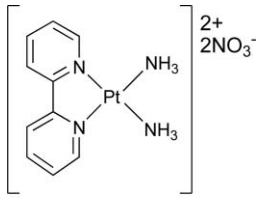

7·2NO$_3$

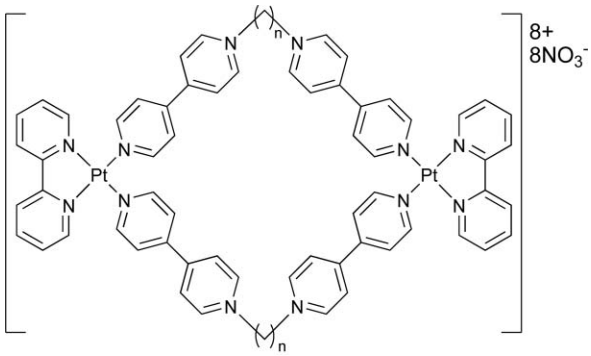

8·8NO$_3$ (n = 4)
9·8NO$_3$ (n = 6)

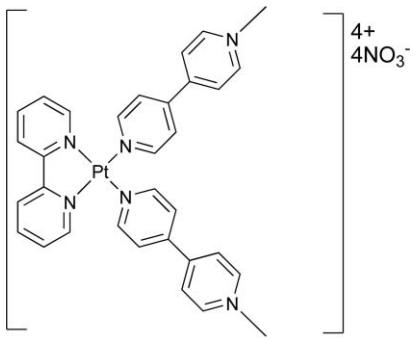

10·4NO$_3$

Results and discussion

Complexes $\mathbf{4}^{2+}$ – $\mathbf{6}^{2+}$ incorporate the hydrophilic, long-chain diamine *O*,*O*′-bis(2-aminoethyl)octadeca(ethylene glycol) (PEGda), while the acyclic diammine complex $\mathbf{7}^{2+}$ was studied as a control compound. PEGda was chosen as the dimensions, functionality and solubility of the resultant large metallomacrocycles $\mathbf{4}^{2+}$ – $\mathbf{6}^{2+}$ are in the range to permit encircling of both ssDNA and dsDNA (~2.5 nm diameter). As Pt(II)-bipyridyl complexes have been reported to interact weakly with DNA by intercalation,[17] $\mathbf{5}^{2+}$ and $\mathbf{6}^{2+}$ were prepared as analogous complexes that lack the bipyridine ligand. The incorporation of *N*,*N*,*N*′,*N*′-tetramethylethylenediamine (tmeda) and ethylenediamine (en) ligands in $\mathbf{5}^{2+}$ and $\mathbf{6}^{2+}$, respectively, would be expected to modulate

the hydrogen-bonding and hydrophobic characteristics of these complexes.

We have reported the design and synthesis of the hexa-bipyridyl complexes $\mathbf{8}^{8+}$ and $\mathbf{9}^{8+}$.[14] These cationic metallomacrocyles are highly water-soluble and provide semi-rigid cavities of different dimensions that are complementary in size to the dimensions of ssDNA. The acyclic complex $\mathbf{10}^{4+}$, which represents approximately one-half of complexes $\mathbf{8}^{8+}$ and $\mathbf{9}^{8+}$, was designed as a control to investigate encircling *versus* surface interactions of the complexes with nucleic acids.

Synthesis

The preparation of complexes $\mathbf{4}\cdot 2NO_3$ – $\mathbf{6}\cdot 2NO_3$ required conditions that would favour the formation of the 62-membered chelate complexes from the flexible diamine PEGda, in preference to linear, cyclic, catenated, bridged and other oligomeric products. While high dilution conditions are often used to promote formation of the thermodynamically-favoured chelate complex, in this study heating solutions of PEGda and suitable metal complex precursors for extended periods, in order to convert any kinetically formed oligomeric intermediates to the desired [1 + 1] macrocycles, allowed the successful preparation of complexes $\mathbf{4}\cdot 2NO_3$ – $\mathbf{6}\cdot 2NO_3$.

The synthesis of $\mathbf{4}\cdot 2NO_3$ was first attempted by mixing a warm aqueous suspension of [Pt(2,2′-bipy)$(NO_3)_2$] and PEGda. However, while the platinum(II) precursor dissolved, the solution became orange-red over time and, upon cooling, a red precipitate formed. The ^{1}H NMR spectrum of the crude product featured resonances exclusively at low field, and suggested the possible formation of a dihydroxo-bridged species [Pt_2(2,2′-bipy)$_2$(μ-OH)$_2$]$(NO_3)_2$. The use of dilute acid (0.01M HNO_3) as the reaction solvent, in order to suppress the formation of any hydroxo species, failed to alter this outcome. However, changing the solvent to DMF (60 °C, 48 h) resulted in a clean, quantitative reaction to give the desired complex $\mathbf{4}\cdot 2NO_3$. The ^{195}Pt NMR spectrum showed a single resonance at –2661 ppm[18] and the ESI-FT-ICR-MS analysis confirmed the presence of $[Pt(2,2'\text{-bipy})(PEGda)]^{2+}$ ions (*m*/*z* 624.29932, calcd 624.30133).

The synthesis of $\mathbf{5}\cdot 2NO_3$ was attempted *via* the labile intermediate $[Pt(tmeda)(OD_2)_2]^{2+}$, which was generated by stirring a warm suspension of [Pt(tmeda)I_2] and $AgNO_3$ in D_2O (70 °C, 48 h). After the removal of insoluble AgI, the colourless solution was added to PEGda and the mixture was heated for a further 48 h. Under these conditions, both ^{1}H and ^{195}Pt{^{1}H} NMR spectroscopic analyses of the filtrate indicated that a mixture of products had formed. However, when dry DMF was used as the solvent the reaction proceeded cleanly to afford $\mathbf{5}\cdot 2NO_3$ in good yield. As with the 2,2′-bipyridine analogue $\mathbf{4}\cdot 2NO_3$, the use of dry DMF is essential to the success of the reaction presumably by ensuring that all intermediates remain soluble during the course of the reaction and/or the curbing of hydrolytic reactions. The analogous $\mathbf{6}\cdot 2NO_3$ was prepared and characterised in a similar manner by using [Pt(en)I_2] as the precursor complex.

Complexes of the type $[Pt(N,N)(PEGda)]^{2+}$ ($\mathbf{4}^{2+}$ – $\mathbf{6}^{2+}$) represent a class of very large metallocyclic compounds. Due to their 62-membered chelate rings, they can be classified as 'gigantocycles', defined by Vögtle[19] as macrocycles having between 50 and 100 atoms in their rings. The complexes also bear close resemblance to simple large aliphatic crown ethers, such as 81-crown-27. The solid state structure of this 81-atom macrocycle shows that the flexible species is twice folded onto itself.[20] It is likely that the PEGda ligands in complexes $\mathbf{4}^{2+}$ – $\mathbf{6}^{2+}$ also exist in similarly folded conformations, which are likely favoured over more open 'extended' states due to entropic and stereoelectronic effects.[21,22]

ESI-MS Experiments

Electrospray ionisation mass spectrometry (ESI-MS) was used to probe the interactions between DNA and complexes $\mathbf{4}^{2+}$ – $\mathbf{7}^{2+}$, $\mathbf{8}^{8+}$, $\mathbf{9}^{8+}$, and $\mathbf{10}^{4+}$. The dsDNA duplex **D2**, which is formed from the two non-self-complementary strands 5′-CCTCATGGCCATGACC-3′ (**D2a**) and 5′-GGTCATGGCCATGAGG-3′ (**D2b**), was chosen as this is a well-studied sequence that has been used to characterize small molecule/DNA interactions by means of ESI-MS.[23] In addition, the strands **D2a** and **D2b** have different masses (4802.0 and 4962.5 Da, respectively, as the protonated form of the phosphodiester) and therefore can provide more information than in the case of self-complementary oligonucleotides where the strands are of equal mass.

The oligonucleotide length of 16 base-pairs was chosen to accommodate the potential binding site size of the largest metallomacrocycle $\mathbf{9}^{8+}$ with DNA, assuming it adopted a fully extended conformation, and also provided an overall negative charge sufficient to neutralise the 8+ charge on each macrocycle that bound to the DNA. In addition, this number of base pairs was included to allow a possible threading mechanism in which the metal complexes could encircle the DNA and allow sufficient residence time of the metal complex-DNA hybrid for detection, prior to any dissociation (unthreading) of the macrocycle. It was presumed that the residence time of such a complex would be very low with only weak interactions holding the adduct together and that its detection would be exceedingly difficult. However, its existence, in equilibrium with other modes of binding, may be reflected in product distributions observed by ESI-MS.

The detection of gas phase ions from DNA solutions in the presence and absence of metal complexes was carried out in the negative-ion mode.[24] As expected, the negative-ion ESI mass spectra of **D2** in both H_2O and 0.1 M NH_4OAc allowed detection of several charge states and a range of $[\mathbf{D2} - nH^+]^{n-}$ ions was observed, with the 6–, 5– and 4– anions being the most abundant. Ions of low abundance assigned to the single-strands $[\mathbf{D2a} - nH^+]^{n-}$ and $[\mathbf{D2b} - nH^+]^{n-}$ were also detected.

Mixtures containing the platinum(II) complexes and either dsDNA **D2** or ssDNA **D2a** were prepared. These experiments typically involved the analysis of freshly-prepared mixtures containing [complex] = [**D2** or **D2a**] = 10 μM (*i.e.* a DNA: complex ratio of 1 : 1) in 0.01 M NH_4OAc (pH 7.0); in some cases 0.1 M NH_4OAc (pH 7.4) was also used.

Interactions with double-stranded DNA

ESI-MS analysis of a mixture containing equimolar amounts of the diplatinum(II) complex $\mathbf{8}^{8+}$ and **D2** showed the formation of 1 : 1 **D2** adducts of the metallomacrocycle, and no evidence of fragment ions derived from $\mathbf{8}^{8+}$. When 2.5 equivalents of the larger metallomacrocycle $\mathbf{9}^{8+}$ were used, ions assigned to two of these cations binding to **D2** were detected. However, at the higher concentration, adducts of fragment ions of $\mathbf{9}^{8+}$ with **D2** were also

observed. The interaction of two molecules of either $\mathbf{8}^{8+}$ or $\mathbf{9}^{8+}$, which have a total charge of 16+, with **D2** (which has an overall charge of 32– in solution) is clearly driven by strong electrostatic interactions.

In order to better understand the effects of size and charge of $\mathbf{8}^{8+}$ and $\mathbf{9}^{8+}$ on DNA-binding, the interactions of **D2** were studied with the mononuclear derivative $\mathbf{10}^{4+}$. The mass spectrum (Fig. 1) featured intense 6– ions arising from free **D2** (*m*/*z* 1626.4) and its 1 : 1 adduct with $\mathbf{10}^{2+}$ (*m*/*z* 1740.0), and the ions of these species in the 5– charge state were prominent. In addition, small amounts of **D2a** and **D2b** were detected, and adducts with $\mathbf{10}^{4+}$ were observed. Low abundance but detectable ions with *m*/*z* values higher than $[\mathbf{D2} + Pt(2,2'\text{-bipy})(Mebipy)_2{}^{4+} - nH^+]^{(n-4)-}$ were also detected. These were assigned to a 1 : 2 adduct, present as both 6– and 5– anions. Formation of a 1 : 2 adduct between the 16-mer DNA and the mononuclear complex $\mathbf{10}^{4+}$ is easily accommodated by the small binding site which spans approximately 3–4 base-pairs, and the overall +4 charge. In contrast, at a 1 : 1 ratio, the larger binding site and the overall charge neutralisation of **D2** upon binding the dinuclear complex $\mathbf{8}^{8+}$ is likely to disfavour the interaction of a second octa-cation with DNA, and the formation of 2 : 1 adducts between $\mathbf{8}^{8+}$ and **D2** were only detected when $\mathbf{8}^{8+}$ was present in excess (2.5 equiv).

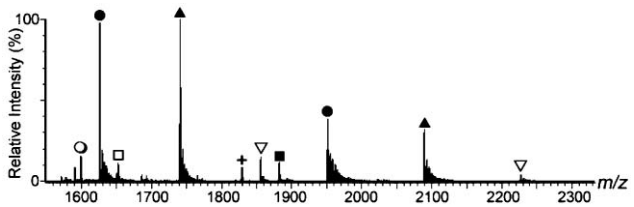

Fig. 1 ESI-MS of **D2** with **10**·4NO$_3$ (1 : 1 in 0.01 M NH_4OAc); ● $[\mathbf{D2} - nH^+]^{n-}$ (n = 4, 5, 6); ○ $[\mathbf{D2a} - 3H^+]^{3-}$; □ $[\mathbf{D2b} - 3H^+]^{3-}$; ▲ $[\mathbf{D2} + Pt(2,2'\text{-bipy})(Mebipy)_2{}^{4+} - nH^+]^{(n-4)-}$ (n = 9, 10); ▽ $[\mathbf{D2} + 2Pt(2,2'\text{-bipy})(Mebipy)_2{}^{4+} - nH^+]^{(n-8)-}$ (n = 13, 14); ✚ $[\mathbf{D2a} + Pt(2,2'\text{-bipy})(Mebipy)_2{}^{4+} - 7H^+]^{3-}$; ■ $[\mathbf{D2b} + Pt(2,2'\text{-bipy})(Mebipy)_2{}^{4+} - 7H^+]^{3-}$.

The ESI mass spectrum of a solution containing equimolar quantities of the PEGda complex $\mathbf{5}^{2+}$ and **D2** is presented in Fig. 2. The high intensity of free **D2** ($[\mathbf{D2} - nH^+]^{n-}$; n = 5, 6) relative to other ions indicated that the binding of **D2** to $\mathbf{5}^{2+}$ is very weak. While the observed intensities of adduct ions were very low, the species $[\mathbf{D2} + Pt(tmeda)(PEGda)^{2+} - nH^+]^{(n-2)-}$ (n = 7, 8) were detected in the gas phase (*m*/*z* 2205.5 and 1837.8 respectively). Similar results were observed with the analogous en complex $\mathbf{6}^{2+}$.

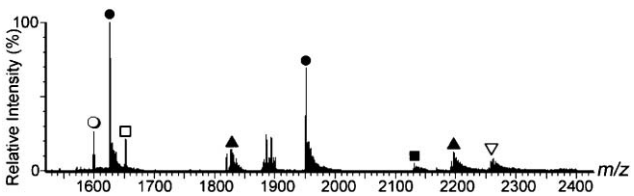

Fig. 2 ESI-MS of **D2** with **5**·2NO$_3$ (1 : 1 in 0.01 M NH_4OAc). Intensities of ions in the ranges *m*/*z* 1800–1900 and 2100–2400 are magnified ×10; ● $[\mathbf{D2} - nH^+]^{n-}$ (n = 5, 6); ○ $[\mathbf{D2a} - 3H^+]^{3-}$; □ $[\mathbf{D2b} - 3H^+]^{3-}$; ▲ $[\mathbf{D2} + Pt(tmeda)(PEGda)^{2+} - nH^+]^{(n-2)-}$ (n = 7, 8); ■ $[\mathbf{D2} + PEGda - 5H^+]^{5-}$; ▽ $[\mathbf{D2} + Pt(tmeda)(PEGda)^{2+} + Pt(tmeda)^{2+} - 9H^+]^{5-}$.

In contrast, no **D2** adducts were detected with the related 2,2′-bipy complex $\mathbf{4}^{2+}$. Ligand dissociation processes involving the PEGda ligand would be somewhat favoured in the case of $\mathbf{4}^{2+}$, in which the π-acceptor bipyridine ligand is known to exert a higher *trans* effect than RNH_2 ligands,[25] leading to fragmentation of the complex prior to DNA binding although no evidence of this process was observed. It is clear from these experiments that the presence of the PEGda ligand in $\mathbf{4}^{2+}$ – $\mathbf{6}^{2+}$ is the most important factor in modulating DNA binding. The acyclic diamine complex $\mathbf{7}^{2+}$ confirmed that the PEGda ligands significantly reduce the relative affinity of $\mathbf{4}^{2+}$ – $\mathbf{6}^{2+}$ for DNA, irrespective of the nature of the smaller chelating ligand. Indeed, complex $\mathbf{7}^{2+}$ exhibited a significant affinity for **D2** at a 1 : 1 molar ratio; ions resulting from two of these dications bound to each duplex were detected, while there was evidence of up to four cations interacting with the duplex **D2** when a 1 : 5 molar ratio was used (Fig. 3; *e.g.* the ion at *m*/*z* 2259.7). The most intense adduct ions were assigned to 1 : 1 species, with ions corresponding to the binding of two, three and four diamine complexes being successively less abundant. While $\mathbf{7}^{2+}$ and the PEGda complexes $\mathbf{4}^{2+}$ – $\mathbf{6}^{2+}$ possess the same overall charge, the large PEGda ligand significantly reduces the formation of DNA adducts observed by ESI-MS presumably by modifying the kinetics of the DNA interaction as the large, macrocyclic ring may adopt some conformation which precludes strong DNA binding. The significant loss of entropy associated with the long, flexible PEG chain and/or steric clashes involving the PEGda ligand may also contribute to the weak DNA binding of $\mathbf{4}^{2+}$ – $\mathbf{6}^{2+}$.

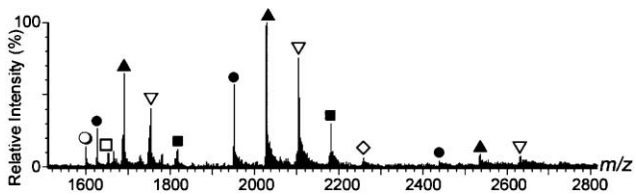

Fig. 3 ESI-MS of **D2** with **7**·2NO$_3$ (1 : 5 in 0.1 M NH_4OAc); ● $[\mathbf{D2} - nH^+]^{n-}$ (n = 4, 5, 6); ○ $[\mathbf{D2a} - 3H^+]^{3-}$; □ $[\mathbf{D2b} - 3H^+]^{3-}$; ▲ $[\mathbf{D2} + Pt(2,2'\text{-bipy})(NH_3)_2{}^{2+} - nH^+]^{(n-2)-}$ (n = 6, 7, 8); ▽ $[\mathbf{D2} + 2Pt(2,2'\text{-bipy})(NH_3)_2{}^{2+} - nH^+]^{(n-4)-}$ (n = 8, 9, 10); ■ $[\mathbf{D2} + 3Pt(2,2'\text{-bipy})(NH_3)_2{}^{2+} - nH^+]^{(n-6)-}$ (n = 11, 12); ◇ $[\mathbf{D2} + 4Pt(2,2'\text{-bipy})(NH_3)_2{}^{2+} - 13H^+]^{5-}$.

Interactions with single-stranded DNA

ESI-MS analysis of an equimolar mixture of **D2a** and **8**·8NO$_3$ (in 0.01 M NH_4OAc) (Fig. 4(a)), showed several peaks. The most intense peak was assigned to **D2a** bound to one dinuclear complex consistent with the high charge and large aromatic surface area of $\mathbf{8}^{8+}$. A 1 : 1 adduct was also observed with the larger metallomacrocycle $\mathbf{9}^{8+}$ (data not shown). Two further species, each present in the 4– and 3– charge states, were identified as the **D2a** adducts of the fragments $[Pt_2(2,2'\text{-bipy})_2\{4,4'\text{-bipy}(CH_2)_4 4,4'\text{-bipy}\}]^{6+}$ and $[Pt(2,2'\text{-bipy})\{4,4'\text{-bipy}(CH_2)_4 4,4'\text{-bipy}\}]^{4+}$, both of which have the potential to bind covalently to **D2a**.

The control experiment with the acyclic complex $\mathbf{10}^{4+}$ showed the presence of several adducts, and up to two intact complexes bound to a single molecule of **D2a** were observed (Fig. 4(b)). This result is in contrast to the corresponding dinuclear complexes $\mathbf{8}^{8+}$ and $\mathbf{9}^{8+}$ in which 1 : 2 adducts were not observed, and is likely a

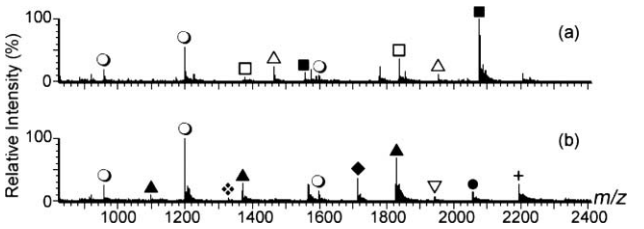

Fig. 4 ESI-MS of **D2a** with equimolar (a) **8**·8NO_3 or (b) **10**·4NO_3 (in 0.01 M NH_4OAc); ○ [**D2a** – $nH^+]^{n-}$ (n = 3, 4, 5); ■ [**D2a** + $Pt_2(2,2'\text{-bipy})_2[4,4'\text{-bipy}(CH_2)_4 4,4'\text{-bipy}]_2^{8+}$ – $nH^+]^{(n-8)-}$ (n = 11, 12); □ [**D2a** + $Pt(2,2'\text{-bipy})[4,4'\text{-bipy}(CH_2)_4 4,4'\text{-bipy}]^{4+}$ – $nH^+]^{(n-4)-}$ (n = 7, 8); △ [**D2a** + $Pt_2(2,2'\text{-bipy})_2[4,4'\text{-bipy}(CH_2)_4 4,4'\text{-bipy}]^{6+}$ – $nH^+]^{(n-6)-}$ (n = 9, 10); ▲ [**D2a** + $Pt(2,2'\text{-bipy})(Mebipy)_2^{4+}$ – $nH^+]^{(n-4)-}$ (n = 7, 8, 9); ● [**D2a** + $2Pt(2,2'\text{-bipy})(Mebipy)_2^{4+}$ – $11H^+]^{3-}$; ◆ [**D2a** + $Pt(2,2'\text{-bipy})^{2+}$ – $nH^+]^{(n-2)-}$ (n = 5, 7); ▽ [**D2a** + $Pt(2,2'\text{-bipy})(Mebipy)_2^{4+}$ + $Pt(2,2'\text{-bipy})^{2+}$ – $9H^+]^{3-}$; ✚ [**D2a** + $2Pt(2,2'\text{-bipy})(Mebipy)_2^{4+}$ + $Pt(2,2'\text{-bipy})^{2+}$ – $13H^+]^{3-}$; ❖ [**D2a** + $Pt(2,2'\text{-bipy})(Mebipy)^{3+}$ – $7H^+]^{4-}$.

result of the differences in charge and also the different dimensions of the mono- and dinuclear complexes which would necessarily occupy different binding sites. Adducts were detected including those containing the fragments $[Pt(2,2'\text{-bipy})]^{2+}$ and $[Pt(2,2'\text{-bipy})(Mebipy)]^{3+}$, suggesting that $[Pt(2,2'\text{-bipy})(Mebipy)_2]^{4+}$ decomposes under the ESI conditions employed. This fragmentation, which was not observed in the analysis of **D2**/**10**$^{4+}$ mixtures, may be due to the increased reactivity of the exposed nucleobases in **D2a** relative to **D2** resulting in the facile displacement of the cationic Mebipy ligands.

ESI-MS analysis of a equimolar mixture of **D2a** and **5**·2NO_3 (0.01 M NH_4OAc) showed intense ions assigned to free **D2a** ([**D2a** – $3H^+]^{3-}$). The only other ion observed was at *m*/*z* 1501, a value consistent with the presence of the adduct [**D2a** + $Pt(tmeda)(PEGda)^{2+}$ – $5H^+]^{3-}$. The low intensity of this ion (relative to that of free **D2a**) suggests that **5**$^{2+}$ has a negligible affinity for **D2a**. Furthermore, neither **4**$^{2+}$ nor **6**$^{2+}$ displayed any evidence of binding to **D2a**.

Comparison of binding affinities with double-stranded DNA

In order to compare the relative DNA-binding strengths of **6**$^{2+}$, **7**$^{2+}$, **9**$^{8+}$ and **10**$^{4+}$ ESI-MS experiments with these complexes were conducted under identical conditions. Due to the low affinity of **6**$^{2+}$ for **D2** (*vide supra*), a 1 : 5 ([**D2**] = 10 μM, [complex] = 50 μM) molar ratio was used for each experiment; complex **8**$^{8+}$ was assessed at a 1 : 2.5 ratio due to the precipitation of an unidentified white solid from solution at higher concentrations (*vide infra*).

A convenient method of comparing DNA-binding is to consider the relative abundances of different DNA/drug adducts.[26] Thus, solutions containing DNA and each compound were prepared in 0.1 M NH_4OAc and subjected to ESI-MS analysis by using a cone voltage = 70 V. The analysis was achieved for each adduct by summing the intensities of ions assigned to this species and dividing by the total intensity of all ions containing **D2** (either free or bound). The ions present in the spectra of double-stranded **D2** were the 5– and 6– ions. The analysis is illustrated below in the case of **10**$^{4+}$ with the ESI mass spectrum given in Fig. 5. Two progressions of 6– and 5– ions were detected, with each ion corresponding to a **D2** molecule bound to between one and four complexes. The relative abundance of, for example, the 1 : 2 adduct,

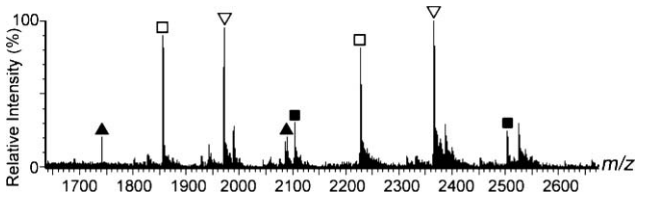

Fig. 5 ESI-MS of **D2** with **10**·4NO_3 (1 : 5 in 0.1 M NH_4OAc); ▲ [**D2** + $Pt(2,2'\text{-bipy})(Mebipy)_2^{4+}$ – $nH^+]^{(n-4)-}$ (n = 9, 10); □ [**D2** + $2Pt(2,2'\text{-bipy})(Mebipy)_2^{4+}$ – $nH^+]^{(n-8)-}$ (n = 13, 14); ▽ [**D2** + $3Pt(2,2'\text{-bipy})(Mebipy)_2^{4+}$ – $nH^+]^{(n-12)-}$ (n = 17, 18); ■ [**D2** + $4Pt(2,2'\text{-bipy})(Mebipy)_2^{4+}$ – $nH^+]^{(n-16)-}$ (n = 21, 22).

was determined by adding the intensities of the 6– and 5– ions of this species (31 and 28 at *m*/*z* 1857.0 and 2228.6, respectively) and dividing by the total intensity of all 6– and 5– ions (156), to give a relative abundance = $^{59}/_{156} \times 100\% = 38\%$. This was repeated for all ions of **D2** (and its adducts) for each mixture. All experiments were also repeated at cone voltages of 90 V, 110 V, 130 V and 150 V.

The DNA-binding of the four platinum(II) complexes was compared to two well-established DNA-binding agents, distamycin A[27] and daunomycin.[28] The naturally-occurring tripeptide distamycin is a well-characterised DNA minor groove binder with a preference for AT tracts, while the antitumour antibiotic, daunomycin interacts preferentially with GC tracts *via* intercalation and minor groove-binding of the daunosamine sugar. While **D2** does not contain a contiguous tract of AT base pairs, distamycin has been previously shown to bind to this sequence.[29]

Fig. 6 shows a plot of the relative abundances of drug/**D2** adducts for **6**$^{2+}$, **7**$^{2+}$, **9**$^{8+}$ and **10**$^{4+}$ as well as distamycin and daunomycin. As expected, distamycin showed a high affinity towards **D2**, and the presence of high intensity ions assigned to 1 : 2 and 1 : 4 adducts is consistent with the reported cooperative binding of two distamycin molecules in the DNA minor groove.[27] Similar results have been reported previously,[29] in which a 1 : 3 **D2**/distamycin mixture (in 0.1 M NH_4OAc) afforded exclusively 1 : 2 adducts in the negative-ion ESI mass spectrum; no 1 : 4 adducts were detected, a result most likely related to the lower molar ratio of distamycin used in their study. Daunomycin also exhibited strong binding to **D2** with adducts containing up to five daunomycin molecules being detected. The distribution of the relevant intensities is very similar to previous studies with other 16-mer duplexes, and is as expected given that the average size of a daunomycin DNA-binding site is three base-pairs.[30,31]

As expected, **6**$^{2+}$ was a weak **D2**-binder, with 1 : 1 adducts being present at 5% relative abundance, and 95% of the assigned ions arising from free **D2**. Complex **7**$^{2+}$ afforded adducts containing up to four cations bound to **D2**, with a much lower relative abundance of free **D2** being observed (21%). Thus, under the conditions used, the PEGda metallomacrocycle **6**$^{2+}$ binds **D2** more weakly to **D2** than the acyclic complex **7**$^{2+}$. For comparison, in the presence of the acyclic tetracation **10**$^{4+}$, no free **D2** was detected, which suggests that **10**$^{4+}$ binds more strongly to **D2** than the diammine complex **7**$^{2+}$. This conclusion was supported by the 1 : 2 and 1 : 3 adducts having greater relative intensities in the case of the bipyridinium complex **10**$^{4+}$. Overall, these results correlate well with charge and aryl surface area, with the relative affinities for **D2** ranked as **6**$^{2+}$ < **7**$^{2+}$ < **10**$^{4+}$.

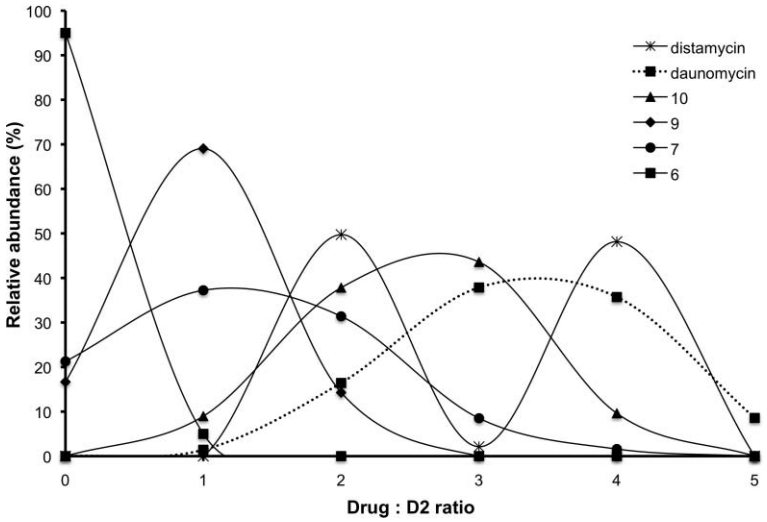

Fig. 6 Plot of relative abundance of drug/**D2** adducts ([**D2**]: [drug] = 1 : 5 for **6**·2NO_3, **7**·2NO_3, and **10**·4NO_3 and 1 : 2.5 for **9**·8NO_3 in 0.1 M NH_4OAc, cone = 70 V).

The binding profile of daunomycin is similar to that for $\mathbf{10}^{4+}$, although it is shifted to a greater number of species being bound to **D2**. Taking into account the detection of ions incorporating up to five daunomycin molecules and the relative intensities of 1 : 4 adducts (36% and 10% for daunomycin and $\mathbf{10}^{4+}$, respectively), daunomycin, not unexpectedly, possesses a higher affinity for **D2** than does the tetracation $\mathbf{10}^{4+}$.

The binding curve for the dinuclear species $\mathbf{9}^{8+}$ was generated using a lower concentration of metal complex due to precipitation of a white solid, presumably the DNA salt of the cation, at higher concentrations. Hence direct comparison of the results with the other curves is not possible. Nevertheless, at a 2.5 : 1 ratio, adducts containing one or two dinuclear species bound to **D2** were observed.

Thermal denaturation experiments

The thermal denaturation of CT-DNA in the presence of platinum(II) complexes was studied using a procedure similar to that described by Cusumano and co-workers.[32] Mixtures of CT-DNA and complexes ([base pairs]/[complex] = 10) were prepared in phosphate-buffered saline solution (pH 7.4) and their thermal denaturation monitored spectrophotometrically over the temperature range 37–100° C. Data were fitted to sigmoidal plots with the maxima of the first derivatives occurring at T_m^c. The data acquired for CT-DNA in the absence of metal complex ($T_m°$) was subtracted from these to obtain ΔT_m. Measurements of all complexes in the absence of DNA showed that these solutions had absorbances which were temperature invariant. The known intercalator ethidium bromide was also used, in order to validate the study and allow for comparison with previously reported results obtained under different conditions.

The results are summarised in Table 1. The free ligand PEGda and the complexes $\mathbf{5}^{2+}$ and $\mathbf{6}^{2+}$ had a negligible effect on the melting of CT-DNA, consistent with very weak interactions with DNA. In contrast, the presence of the 2,2′-bipy ligand in the metallomacrocycle $\mathbf{4}^{2+}$ resulted in stabilisation of DNA, as evidenced by ΔT_m of 5.8 °C. The related diammine species $\mathbf{7}^{2+}$ resulted in a comparable increase in the DNA melting temperature (ΔT_m = 5.4 °C). These data are consistent with the ESI-MS results and indicate the important contribution of the 2,2′-bipy ligand in DNA-binding.

Table 1 Changes in the melting temperature (ΔT_m) of CT-DNA in the presence of selected compounds

Compound	ΔT_m/°C
PEGda	–0.7
6·2NO_3	0.6
5·2NO_3	0.8
7·2NO_3	5.4
4·2NO_3	5.8
10·4NO_3	11.3
Ethidium bromide	12.6
9·8NO_3	25.5

Given the substantial length of CT-DNA (>20,000 base-pairs), encircling of DNA by the PEGda bound ligands would likely not occur. The PEGda ligands could, however, participate in non-specific van der Waals interactions as well as H-bonding interactions between the *O*-atoms and nucleobase H-donor sites, *e.g.* the exocyclic amino groups of G and A. Such interactions would require the PEGda ligand to adopt a conformation that positioned these atoms near the major and/or minor grooves. The thermal denaturation data suggest that these interactions, if present, are very weak and do not contribute significantly to the stabilisation of DNA.

In contrast to the complexes of PEGda, the dinuclear metallocycle $\mathbf{9}^{8+}$ resulted in a marked increase in the stability of dsDNA (ΔT_m = 25.5 °C). The high charge of the dinuclear complex, as well as its large aromatic surface area undoubtedly contribute to strong DNA binding. The tetra-cation $\mathbf{10}^{4+}$ also stabilised dsDNA (ΔT_m = 11.3 °C) and gave a change in melting temperature comparable to that of ethidium bromide (ΔT_m = 12.6 °C), but a significantly lower value than for the dinuclear species $\mathbf{9}^{8+}$. This difference is consistent with the reduced size and charge of $\mathbf{10}^{4+}$, relative to that of the dinuclear complex $\mathbf{9}^{8+}$.

Conclusion

The interactions of cationic platinum(II) metallomacrocyles with single- and double-stranded 16-mer oligonucleotides analysed by means of ESI-MS has been contrasted with their ability to stabilise bulk CT-DNA in solution using thermal denaturation measurements. Both the ESI-MS and thermal denaturation studies of mononuclear platinum(II) complexes containing a 62-membered chelate of PEGda were consistent with their very low affinities for nucleic acids. While the PEGda macrocycle is highly flexible, and has dimensions compatible for encircling both double- and single-stranded DNA, under the conditions used in the ESI-MS experiments there was no evidence for the macrocycle binding to either ssDNA or dsDNA by means of a topological interaction. In contrast, the bipyridinium complexes $\mathbf{9}^{8+}$ and $\mathbf{10}^{4+}$ interact strongly with both ssDNA and dsDNA, a result attributed to their greater number of aryl groups and high overall positive charge. The increase in melting temperature of CT-DNA by the metallomacrocycle $\mathbf{9}^{8+}$ parallels increases observed by strong DNA binders such bis-intercalators.[33,34] While the nature of the binding modes cannot be determined from the experimental results, the stoichiometries of the adducts detected between the 16-mer DNA and $\mathbf{9}^{8+}$ suggest that the macrocyclic cavity adopts a conformation that elongates the complex to cover approximately eight base-pairs and allows effective neutralisation of the positive charge by the DNA phosphodiester backbone. Further functionalisation of the pyridyl-alkyl-pyridyl coordinating units to include hydrogen bond donor/acceptor groups and or increased hydrophobicity may further modulate the DNA binding characteristics of the complexes.

Experimental

For all ligands, low resolution ESI-MS data were collected using a Finnigan LCQ detector. For all new complexes, high resolution ESI-FT-ICR-MS data were collected using either a Bruker 7.0T or a Bruker Apex 4.7T spectrometer. NMR spectra were recorded at 300 K using a Bruker Avance DPX300 or DPX400 spectrometer. Unless otherwise stated: chemical shifts (δ) are reported relative to TMS and were referenced to residual solvent signals; data for ^{1}H, ^{13}C{^{1}H} (data in D_2O uncalibrated) and ^{195}Pt (relative to external $Na_2[PtCl_4]$ at −1628 ppm) nuclei were recorded at 300, 75 and 85 MHz, respectively. UV-vis data were recorded using a Varian Cary 500 spectrophotometer (equipped with a Cary temperature controller).

Unless otherwise stated, all chemicals used were obtained from commercial sources and were used without further purification. All solid materials were dried (P_2O_5) under vacuum for at least 24 h prior to use. The compound PEGda (Fluka, oligomeric purity) contained trace impurities, as evidenced by ESI-MS, *e.g.* *O*,*O*′-bis(aminoethyl)heptadeca(ethylene glycol) could be detected (*m*/*z* 854 $[M + H^+]^+$). Complexes $\mathbf{8}\cdot 8NO_3$ and $\mathbf{9}\cdot 8NO_3$ were prepared as described previously.[14]

The 16-mers **D2a**, **D2b** (Geneworks, HPLC grade) were purified using HPLC (aqueous $NH_4OAc \rightarrow MeCN$ gradient) as reported previously.[35] In each case, equimolar quantities[36] of the appropriate strands (both dissolved in 0.1 M NH_4OAc, pH 7.4) were combined to give a mixture in which the concentration of each of these constituents was 1 mM (values for [ssDNA] were estimated by measurement of UV absorbance at 260 nm using ε_{260} values for A, G, C and T of 15200, 12010, 7050 and 8400 $M^{-1}cm^{-1}$, respectively).[36] This solution was heated at (T_m + 20) °C and cooled slowly to room temperature to afford a stock solution of the annealed dsDNA, which was used without further purification. CT-DNA (sodium salt, highly polymerised) was re-suspended in phosphate-buffered saline solution (1 mM phosphate, 2 mM NaCl, pH 7.4) and its concentration was determined spectrophotometrically.[37] CT-DNA concentration, quantified as [base-pairs], was estimated using ε_{260} = 13100 $M_{base\text{-}pairs}^{-1}$ cm^{-1}.[37] MilliQ™ H_2O was used for all experiments requiring H_2O.

Synthesis

[Mebipy]NO_3. [Mebipy]I[38] (1.490 g, 5.00 mmol) was dissolved in H_2O (5 mL), and treated with $AgNO_3$ (0.849 g, 5.00 mmol) in H_2O (5 mL). The mixture was filtered and concentrated to ~3 mL on a hotplate. Slow evaporation of the reaction mixture afforded the title compound as colourless crystals (0.361 g, 31%). ^{1}H NMR (D_2O) δ 8.92 (d, 2H, $^{3}J_{H,H}$ = 6.76 Hz, H2), 8.72 (d, 2H, $^{3}J_{H,H}$ = 4.43 Hz, H2′), 8.36 (d, 2H, $^{3}J_{H,H}$ = 6.76 Hz, H3), 7.87 (d, 2H, $^{3}J_{H,H}$ = 6.76 Hz, H3′), 4.47 (s, 3H, CH_3) ppm. ^{13}C{^{1}H} NMR (D_2O) δ 153.72, 150.37, 146.02, 142.86, 126.04, 122.79, 48.23 ppm. ESI-MS: *m*/*z* 171.00 $[M - NO_3^-]^+$. Anal. Calc. for $C_{11}H_{11}N_3O_3$: C, 56.65; H, 4.75; N, 18.02. Found: C, 56.94; H, 4.99; N, 18.30.

[Pt(2,2′-bipy)(PEGda)]$(NO_3)_2$ (4·2NO_3). [Pt(2,2′-bipy)-$(NO_3)_2$][39] (10.6 mg, 22.4 μmol) and PEGda (20.1 mg, 22.4 μmol) were dissolved in DMF (5 mL) and stirred for 48 h at 60 °C after which the yellow solution was evaporated to dryness. The oily residue was dissolved in H_2O (1 mL) and the mixture filtered through cellulose to afford a stock solution of the title complex. ^{1}H NMR (DMF-d_7) δ 9.11 (d, 2H, $^{3}J_{H,H}$ = 5.63 Hz, $H6_{bipy}$), 8.90 (d, 2H, $^{3}J_{H,H}$ = 7.55 Hz, $H3_{bipy}$), 8.66 (m, 2H, $H4_{bipy}$), 8.07 (m, 2H, $H5_{bipy}$), 6.46 (br, s, 4H, NH_2), 4.00-3.40 (m, 76H, $(CH_2OCH_2)_{19}$), 3.36 (m, 4H, CH_2NH_2) ppm. ^{195}Pt NMR (DMF-d_7) δ −2660.6. ESI-FT-ICR-MS: *m*/*z* calcd for $C_{50}H_{92}N_4O_{19}Pt^{2+}$, $[M - 2NO_3^-]^{2+}$: 624.30133. Found: 624.29932.

[Pt(tmeda)(PEGda)]$(NO_3)_2$ (5·2NO_3). [Pt(tmeda)I_2][40] (15.9 mg, 28.2 μmol) was suspended in DMF (3 mL) and treated with $AgNO_3$ (9.54 mg, 56.2 μmol) in DMF (3 mL). The mixture was stirred in the absence of light for 24 h at 55 °C. AgI was removed by filtration, and the colourless filtrate was added to PEGda (25.3 mg, 28.2 μmol). The solution was stirred for 72 h at 55 °C, after which it was evaporated to dryness. The oily residue was dissolved in H_2O (1 mL) and the mixture filtered through cellulose to afford a stock solution of the title complex. ^{1}H NMR (DMF-d_7) δ 5.51 (br, s, 4H, NH_2), 4.00-3.40 (m, 76H, $(CH_2OCH_2)_{19}$), 3.30 (m, 4H, CH_2NH_2), 2.97 (s, 12H, CH_3(tmeda)), 2.90 (s, 4H, CH_2(tmeda)). ^{195}Pt NMR (DMF-d_7) δ − 2695.5. ESI-FT-ICR-MS: *m*/*z* calcd for $C_{46}H_{100}N_5O_{22}Pt^+$, $[M - NO_3^-]^+$: 1269.65022. Found: 1269.64911.

[Pt(en)(PEGda)]$(NO_3)_2$ (6·2NO_3). [Pt(en)I_2][40] (13.40 mg, 26.33 μmol) was suspended in DMF (3 mL) and treated with $AgNO_3$ (8.88 mg, 52.26 μmol) in DMF (3 mL). The mixture was stirred in the absence of light for 24 h at 55 °C. AgI was removed by filtration, and the colourless filtrate was added to PEGda (23.61 mg, 26.33 μmol) in DMF (1 mL). The solution

was stirred for 72 h at 55 °C, after which it was evaporated to dryness to give a pale yellow oil which was used without further purification. ^{1}H NMR (DMF-d_7) δ 5.72 (br, s, 4H, NH_2), 5.44 (br, s, 4H, NH_2), 3.90–3.40 (m, 76H, $(CH_2OCH_2)_{19}$), 3.03 (m, 4H, CH_2NH_2), 2.75 (br, s, 4H, CH_2(en)). ^{195}Pt NMR (DMF-d_7) δ –2870 ppm. ESI-FT-ICR-MS: m/z calcd for $C_{42}H_{92}N_5O_{22}Pt^+$, [M – NO_3^-]$^+$: 1213.58762. Found: 1213.58575.

[Pt(2,2′-bipy)(NH$_3$)$_2$](NO$_3$)$_2$ (7·2NO$_3$). [Pt(2,2′-bipy)$(NO_3)_2$][39] (18.25 mg, 38.4 μmol) was suspended in H_2O (0.3 mL) and treated with aqueous NH_3 (28% solution, 26 mg, ~430 μmol). The suspension was stirred for 4 h at 70 °C and allowed to cool. The mixture was filtered through cellulose, and the resulting pale-yellow solution was allowed to evaporate slowly to give the product as a pale yellow powder (16.9 mg, 86%). ^{1}H NMR (DMSO-d_6) δ 8.71 (m, 4H, H3, H6), 8.53 (m, 2H, H4), 7.96 (m, 2H, H5), 5.28 (br, s, 6H, NH_3). ^{13}C{^{1}H} NMR (DMSO-d_6) δ 156.4, 149.5, 141.8, 127.8, 124.6. ^{195}Pt NMR (DMSO-d_6) δ –2604. ESI-FT-ICR-MS: m/z calcd for $C_{20}H_{28}N_{11}O_9Pt_2^+$, [2M – NO_3^-]$^+$: 956.13615. Found: 956.13360. Anal. calcd for $C_{10}H_{14}N_6O_6Pt$: C, 23.58; H, 2.77; N, 16.50. Found: C, 23.77; H, 2.91; N, 16.51.

[Pt(2,2′-bipy)(Mebipy)$_2$](NO$_3$)$_4$ (10·4NO$_3$). This complex has been reported previously as its perchlorate salt.[41] [Pt(2,2′-bipy)$(NO_3)_2$][39] (15.0 mg, 38.8 μmol) was added to a solution of 1-methyl-4,4′-bipyridinium nitrate (18.1 mg, 77.6 μmol) in H_2O (0.5 mL) and the suspension was stirred overnight at 80 °C, over which time [Pt(2,2′-bipy)$(NO_3)_2$] had dissolved. The pale-yellow solution was filtered through cellulose, and slowly evaporated to give the product as a pale-yellow powder (97%). ^{1}H NMR (D_2O) δ 9.44 (dd, 4H, $^3J_{H,H}$ = 5.51 Hz, $^4J_{H,H}$ = 1.33 Hz, $H2_{Mebipy}$), 9.02 (d, 4H, $^3J_{H,H}$ = 6.79 Hz, $H2'_{Mebipy}$), 8.57 (d, 2H, $^3J_{H,H}$ = 7.44 Hz, $H6_{bipy}$), 8.51 (obscured, 2H, $H4_{bipy}$), 8.48 (d, 4H, $^3J_{H,H}$ = 6.79 Hz $H3'_{Mebipy}$), 8.28 (dd, 4H, $^3J_{H,H}$ = 5.51 Hz, $^4J_{H,H}$ = 1.33 Hz, $H3_{Mebipy}$), 7.82 (d, 2H, $^3J_{H,H}$ = 5.50 Hz, $H5_{bipy}$), 7.70 (td, 2H, $^3J_{H,H}$ = 7.40 Hz, $^4J_{H,H}$ = 1.33 Hz $H5_{bipy}$), 4.52 (s, 3H, CH_3). ^{13}C{^{1}H} NMR (100 MHz, D_2O) δ 156.9, 153.3, 150.8, 149.5, 146.8, 146.1, 142.8, 128.2, 126.8, 126.2, 124.4, 48.2. ^{195}Pt NMR (D_2O) δ –2523. ESI-MS: m/z 879.64 [M – NO_3^-]$^+$; 1944 [2M + NO_3^-]$^-$, 1003.02 [M + NO_3^-]$^-$. Anal. calcd for $C_{32}H_{30}N_{10}O_{12}Pt·3.5H_2O$: C, 38.25; H, 3.71; N, 13.94. Found: C, 38.09; H, 3.41; N, 13.77.

ESI-MS studies involving DNA

Freshly prepared stock solutions of DNA (1 mM in 0.1 M NH_4OAc) and metal complexes (200 μM in either 0.01 or 0.1 M NH_4OAc) were prepared. These were combined and diluted with either 0.01 or 0.1 M NH_4OAc to give mixtures in which the final concentration of DNA was 10 μM (pH ≈ 7.0 or 7.4 for 0.01 and 0.1 M NH_4OAc, respectively). The solutions were mixed by vortexing and left at room temperature for at least 15 min before being analysed. Negative-ion ESI mass spectra were acquired using a Waters Q-ToF Ultima mass spectrometer equipped with a Z-spray probe, calibrated over the appropriate range with CsI (750 μM). Unless otherwise stated, the conditions used were: $V_{capillary}$ = 2.5 V, V_{cone} = 70 V, T_{source} = 25 °C, $T_{desolvation}$ = 100 °C, collision energy = 2. Spectra were acquired by summing 20 scans (10 scans for the comparative binding studies of **D2**).

Thermal denaturation studies

Thermal denaturation experiments of DNA in the presence of metal complexes were performed using a procedure similar to that employed by Cusumano and co-workers.[32] Mixtures of CT-DNA and complexes ([DNA base pairs] = 78 μM, [complex] = 7.8 μM) were prepared in phosphate-buffered saline solution (1 mM phosphate, 2 mM NaCl, pH 7.4) and their thermal denaturation monitored by recording absorbance values at 260 nm over the temperature range 37–100 °C. The solutions were held at 37° C for 30 min prior to heating at 0.5 °C min^{-1} and absorbance readings were taken every 2 min (1° C). Data were fitted to sigmoidal plots using Origin 7.0®, and T_m values were estimated from the x-intercepts of 2nd derivative plots. All values are averaged over at least two runs for each mixture. These were compared to values obtained for CT-DNA in the absence of metal complex.

Acknowledgements

We thank Dr Ian Luck (The University of Sydney) for assistance with the NMR experiments and Dr Keith Fisher (The University of Sydney) for assistance with the ESI-MS experiments. We also thank Johnson Matthey for the loan of $K_2[PtCl_4]$. Financial support from the Australian Research Council (DP Grant #DP0557235) is gratefully acknowledged (MMH & LMR).

References

1 D. R. Boer, A. Canals and M. Coll, *Dalton Trans.*, 2009, 399–414.
2 G. Damia and M. Broggini, *Drugs Future*, 2005, **30**, 301–309.
3 J. B. Chaires and J.-L. Mergny, *Biochimie*, 2008, **90**, 973–975.
4 R. Palchaudhuri and P. J. Hergenrother, *Curr. Opin. Biotechnol.*, 2007, **18**, 497–503.
5 I. Kostova, *Curr. Med. Chem.*, 2006, **13**, 1085–1107.
6 P. J. Dyson and G. Sava, *Dalton Trans.*, 2006, 1929–1933.
7 A. Oleksi, A. G. Blanco, R. Boer, I. Us, J. Aymam, A. Rodger, M. J. Hannon and M. Coll, *Angew. Chem., Int. Ed.*, 2006, **45**, 1227–1231.
8 M. Mounir, J. Lorenzo, M. Ferrer, M. J. Prieto, O. Rossell, F. X. Aviles and V. J. Moreno, *J. Inorg. Biochem.*, 2007, **101**, 660–666.
9 R. Kieltyka, P. Englebienne, J. Fakhoury, C. Autexier, N. Moitessier and H. F. Sleiman, *J. Am. Chem. Soc.*, 2008, **130**, 10040–10041.
10 N. W. Kim, M. A. Piatyszek, K. R. Prowse, C. B. Harley, M. D. West, P. L. C. Ho, G. M. Coviello, W. E. Wright, R. L. Weinrich and J. W. Shay, *Science*, 1994, **266**, 2011–2015.
11 M. A. Galindo, S. Galli, J. A. R. Navarro and M. A. Romero, *Dalton Trans.*, 2004, 2780–2785.
12 M. A. Galindo, D. Olea, M. A. Romero, J. Gomez, P. del Castillo, M. J. Hannon, A. Rodger, F. Zamora and J. A. R. Navarro, *Chem.–Eur. J.*, 2007, **13**, 5075–5081.
13 D. Ghosh, H. Ahmad and J. A. Thomas, *Chem. Commun.*, 2009, 2947–2949.
14 D. Schilter, J. K. Clegg, M. M. Harding and L. M. Rendina, *Dalton Trans.*, 2010, **39**, 239–247.
15 M. M. Hingorani and M. O'Donnell, *Curr. Biol.*, 1998, **8**, R83–R86.
16 X.-P. Kong, R. Onrust, M. O'Donnell and J. Kuriyan, *Cell*, 1992, **69**, 425–437.
17 M. Casumano, M. L. Di Pietro, A. Giannetto and P. A. Vainiglia, *J. Inorg. Biochem.*, 2005, **99**, 560–565.
18 J. R. L. Priqueler, I. S. Butler and F. D. Rochon, *Appl. Spectrosc. Rev.*, 2006, **41**, 185–226.
19 V. Prautzsch, S. Ibach and F. J. Vögtle, *J. Inclusion Phenom. Macrocyclic Chem.*, 1999, **33**, 427–458.
20 Z. Yang, G.-E. Yu, J. Cooke, Z. Ali-Adib, K. Viras, H. Matsuura, A. J. Anthony and C. Booth, *J. Chem. Soc., Faraday Trans.*, 1996, **92**, 3173–3182.
21 T. P. Straatsma and J. A. McCammon, *J. Chem. Phys.*, 1989, **91**, 3631–3637.

22 N. A. Al-Jallal, A. A. Al-Kahtani and A. A. El-Azhary, *J. Phys. Chem. A*, 2005, **109**, 3694–3703.
23 T. Urathamakul, J. L. Beck, M. M. Sheil, J. R. Aldrich-Wright and S. F. Ralph, *Dalton Trans.*, 2004, 2683–2690.
24 J. L. Beck, M. L. Colgrave, S. F. Ralph and M. M. Sheil, *Mass Spectrom. Rev.*, 2001, **20**, 61–87.
25 N. Summa, W. Schiessl, R. Puchta, N. van Eikema Hommes and R. van Eldik, *Inorg. Chem.*, 2006, **45**, 2948–2959.
26 J. L. Beck, R. Gupta, T. Urathamakul, N. L. Williamson, M. M. Sheil, J. R. Aldrich-Wright and S. F. Ralph, *Chem. Commun.*, 2003, 626–627.
27 P. B. Dervan, A. T. Poulin-Kerstien, E. J. Fechter and B. S. Edelson, *Top. Curr. Chem.*, 2005, **253**, 1–31.
28 J. B. Chaires, *Small Mol. DNA RNA Binders*, 2003, **2**, 461–481.
29 R. Gupta, J. L. Beck, S. F. Ralph, M. M. Sheil and J. R. Aldrich-Wright, *J. Am. Soc. Mass Spectrom.*, 2004, **15**, 1382–1391.
30 T. Urathamakul, J. L. Beck, M. M. Sheil, J. R. Aldrich-Wright and S. F. Ralph, *Dalton Trans.*, 2004, 2683–2690.
31 L. E. Xodo, G. Manzini, J. Ruggiero and F. Quadrifoglio, *Biopolymers*, 1988, **27**, 1839–1857.
32 M. Cusumano, M. L. Di Pietro and A. Giannetto, *Inorg. Chem.*, 2006, **45**, 230–235.
33 B. B. Hasinoff, R. Zhang, X. Wu, L. J. Guziec, F. S. Guziec, K. Marshall and J. C. Yalowich, *Bioorg. Med. Chem.*, 2009, **17**, 4575–4582.
34 J. Portugal, D. J. Cashman, J. O. Trent, N. Ferrer-Miralles, T. Przewloka, I. Fokt, W. Priebe and J. B. Chaires, *J. Med. Chem.*, 2005, **48**, 8209–8219.
35 G. Wickham, P. Iannitti, J. Boschenok and M. M. Sheil, *J. Mass Spectrom.*, 1995, **30**, S197–S203.
36 W. A. Kibbe, *Nucleic Acids Res.*, 2007, **35**, W43–W46.
37 R. D. Wells, J. E. Larson, R. C. Grant, B. E. Shortle and C. R. Canton, *J. Mol. Biol.*, 1970, **54**, 465–497.
38 B. J. Coe, M. C. Chamberlain, J. P. Essex-Lopresti, S. Gaines, J. C. Jeffery, S. Houbrechts and A. Persoons, *Inorg. Chem.*, 1997, **36**, 3284–3292.
39 S. Wimmer, P. Castan, F. L. Wimmer and N. P. Johnson, *J. Chem. Soc., Dalton Trans.*, 1989, 403–412.
40 M. J. Arendse, G. K. Anderson and N. P. Rath, *Inorg. Chem.*, 1999, **38**, 5864–5869.
41 K. Sakai, M. Osada, Y. Yokoyama, Y. Tomita and T. Tsubomura, *Acta Crystallogr., Sect. E: Struct. Rep. Online*, 2003, **E59**, m512–m514.